Developmental Biology **222,** 376–391 (2000)
doi:10.1006/dbio.2000.9717, available online at http://www.idealibrary.com on IDEAL®

The bHLH Class Protein pMesogenin1 Can Specify Paraxial Mesoderm Phenotypes

Jeong Kyo Yoon,* Randall T. Moon,† and Barbara Wold*,[1]

**Division of Biology, 156-29, California Institute of Technology, Pasadena, California 91125; and †Howard Hughes Medical Institute, Department of Pharmacology, and Center for Developmental Biology, University of Washington School of Medicine, Room K536C, Health Sciences Building, Campus Box 357750, Seattle, Washington 98195*

A new bHLH gene from mouse that we call *pMesogenin1* (referring to paraxial mesoderm-specific expression and regulatory capacities) and its candidate ortholog from *Xenopus* were isolated and studied comparatively. In both organisms the gene is specifically expressed in unsegmented paraxial mesoderm and its immediate progenitors. A striking feature of *pMesogenin1* expression is that it terminates abruptly in presumptive somites (somitomeres). Somitomeres rostral to the *pMesogenin1* domain strongly upregulate expression of *pMesogenin's* closest known paralogs, *MesP1* and *MesP2* (*Thylacine1/2* in *Xenopus*). Subsequently, the most rostral somitomere becomes a new somite and expression of *MesP1/2* is sharply downregulated before this transition. Thus, expression patterns of these bHLH genes, together with that of an additional bHLH gene in the mouse, *Paraxis*, collectively define discrete but highly dynamic prepatterned subdomains of the paraxial mesoderm. In functional assays, we show that *pMesogenin1* from either mouse or frog can efficiently drive nonmesodermal cells to assume a phenotype with molecular and cellular characteristics of early paraxial mesoderm. Among genes induced by added *pMesogenin1* is *Xwnt-8*, a signaling factor that induces a similar repertoire of marker genes and a similar cellular phenotype. Additional target genes induced by *pMesogenin1* are *ESR4/5*, regulators known to play a significant role in segmentation of paraxial mesoderm (W. C. Jen *et al.*, 1999, *Genes Dev.* 13, 1486–1499). *pMesogenin1* differs from other known mesoderm-inducing transcription factors because it does not also activate a dorsal (future axial) mesoderm phenotype, suggesting that *pMesogenin1* is involved in specifying paraxial mesoderm. In the context of the intact frog embryo, ectopic *pMesogenin1* also actively suppressed axial mesoderm markers and disrupted normal formation of notochord. In addition, we found evidence for cross-regulatory interactions between *pMesogenin1* and T-box transcription factors, a family of genes normally expressed in a broader pattern and known to induce multiple types of mesoderm. Based on our results and results from prior studies of related bHLH genes, we propose that *pMesogenin1* and its closest known relatives, *MesP1/2* (in mouse) and *Thylacine1/2* (in *Xenopus*), comprise a bHLH subfamily devoted to formation and segmentation of paraxial mesoderm.

Key Words: **bHLH gene; MesP1; MesP2; Thylacine; paraxial mesoderm; somitomeres; somite; *Xenopus laevis;* mouse.**

INTRODUCTION

Paraxial mesoderm in vertebrate embryos gives rise to all future trunk and limb skeletal muscles, the entire trunk skeleton, and portions of the trunk dermis and vasculature (Christ and Ordahl, 1995; Tam and Trainor, 1994). A unique characteristic of paraxial mesoderm in vertebrate embryos is the formation of the somite, which is the primary morphogenetic event in segmentation (reviewed in Gossler and de Angelis, 1998; Tam and Trainor, 1994). Segmentation of the trunk musculoskeletal system arises directly from the segmentation of the paraxial mesoderm. Paraxial mesoderm of both mouse and chicken originates from the presumptive mesodermal cells that migrate through the primitive streak during gastrulation (Lawson and Pedersen, 1992; Smith and Schoenwolf, 1998; Tam and Beddington, 1992). In frogs the process is not identical but it is analogous. Presumptive mesodermal cells, including the cells of the future paraxial mesoderm, migrate during gastrulation through the involuting marginal zone of the embryo that is functionally equivalent to the primitive streak (Beddington,

[1] To whom correspondence should be addressed. Fax: (626) 449-0756.

0012-1606/00 $35.00

1993). Shortly after gastrulation, paraxial mesodermal cells form two unsegmented columns of tissue positioned laterally on either side of the neural tube and oriented parallel to it. As development proceeds, these columns are segmented in a stepwise manner beginning at the rostral end and proceeding caudally to form two identical strings of somites (Christ and Ordahl, 1995; Gossler and de Angelis, 1998). The caudal portion of paraxial mesoderm that is not yet segmented is called presomitic paraxial mesoderm (PSM; also segmental plate in the chick embryo or tailbud in the later embryonic stages).

The PSM is a highly dynamic structure in which new somites bud into existence continually at the rostral boundary, and at the caudal end new mesoderm cells continue to join, thereby providing new tissue to support continued trunk and tail growth (Tam and Trainor, 1994). As development proceeds in both mouse and chicken, the wavefront of new somite formation advances caudally. Just before cells of the PSM are segregated into a new somite, they undergo a mesenchymal/epithelial transition. A newly formed somite is then budded from the rostral end of the presomitic mesoderm as an epithelial ball with a relatively constant, species-specific rate as somitogenesis progresses (Tam and Trainor, 1994). As somites mature, again in a rostrocaudal gradient that shadows the gradient of somite formation, they are further patterned by multiple signaling interactions with adjacent tissues. This ultimately leads to irreversible cell fate specification and differentiation into diverse cell types (Cossu *et al.,* 1996; Yun and Wold, 1996). In frogs, somites are also formed under the same basic plan, in a rostral–caudal gradient from unsegmented paraxial mesoderm, although somitogenesis itself does not involve a mesenchymal epithelial transition (Jen *et al.,* 1997).

From the current level of knowledge, four major regulatory events can be discerned in the life of a paraxial mesoderm cell prior to its incorporation into a new somite: (1) Presumptive paraxial mesoderm progenitor cells move through the primitive steak in birds and mammals and through the blastopore in amphibians (Beddington, 1993; Tam, 1998). (2) Paraxial mesoderm cells are specified and become distinguishable at the level of gene expression from other mesodermal progenitors during gastrulation (Tam, 1998). (3) A cellular "molecular clock," which is widely thought to be central for regulating segmentation, is set within cells of the unsegmented paraxial mesoderm as they join its caudal end (Cooke, 1998; Jiang *et al.,* 1998; Palmeirim *et al.,* 1997). (4) Mesenchymal paraxial mesoderm cells become prepatterned into presumptive somites (sometimes called somitomeres), as revealed by expression of genes such as *MesP1/2* of mouse and their apparent orthologs *Thylacine1/2* of frog (Saga *et al.,* 1996, 1997; Sparrow *et al.,* 1998). Formation of a new somite is concurrent with another set of sharp changes in the repertoire of genes expressed.

In *Xenopus,* mesoderm specification and some subsequent mesoderm development and differentiation can be achieved experimentally without gastrulation using an isolated "animal cap" assay (Dawid, 1991). Intensive studies of this type over the past decade have identified a number of genes that can broadly initiate mesoderm formation in dissected animal caps, a portion of the blastula which would otherwise produce only ectodermal derivatives. Many of the most potent inducers of mesoderm in this system are signaling molecules that act upstream, in developmental terms, of transcriptional regulators that specify the expression of mesoderm genes (Smith, 1995). Among these signals, Activin, a member of the TGFβ family, induces panmesodermal tissues, while FGF and Xwnt-8 induce ventral/lateral mesodermal tissues. Ectopic expression of T-box transcription factors, including *Xbra* and *Eomesodermin,* in animal caps also produces diverse mesodermal derivatives that include paraxial mesoderm and axial mesoderm (notochord) (Ryan *et al.,* 1996; Smith, 1995).

bHLH and HLH transcription factors are central components in transcriptional regulatory networks known to govern specification and differentiation in diverse tissues. Skeletal myogenesis is the classic case in which the four-member MyoD family is well known for its role in regulating cell fate determination and cellular differentiation (Yun and Wold, 1996). Other bHLH regulators are expressed prominently at earlier times in the mesodermal lineage that ultimately leads to skeletal muscle as well as other mesodermal derivatives. Several of these genes appear to be important for somitogenesis. For example, mutation of the bHLH gene *Paraxis* disrupts the formation of epithelial somites, although the essential features of segmentation and establishment of somitic cell lineages remain remarkably intact (Burgess *et al.,* 1996). *MesP1/2* of the mouse (or *Thylacine1/2* in *Xenopus*) are expressed very transiently in the somitomeric domain shortly before it is separated from the block of unsegmented paraxial mesoderm, and mutation of both genes disrupts somite segmentation (Saga *et al.,* 1997; Sparrow *et al.,* 1998). This led us to think that additional bHLH family members would likely be important in earlier stages of paraxial mesoderm specification or segmentation.

We report here the isolation and characterization of a new mouse gene, *pMesogenin1,* together with its apparent *Xenopus* ortholog. These genes code for a bHLH class transcription factor whose apparent paralogs are *MesP1/2* in the mouse and *Thylacine1/2* in the frog. We present a comparative study in mouse and frog which shows that *pMesogenin1* RNA is expressed specifically in presomitic paraxial mesoderm and its immediate presumptive progenitor cells in both animals and suggests that they are orthologous genes. The spatiotemporal domains of *pMesogenin1* expression are then defined with higher resolution relative to other pertinent bHLH and T-box regulators of mesoderm specification and of somitogenesis. Finally, the current study examines the functional effects of *pMesogenin1* expression on mesoderm specification. A model is proposed in which *pMesogenin1* and *MesP1/2* (in mouse) or *Thylacine1/2* (in *Xenopus*) comprise a bHLH subfamily devoted to formation and segmentation of paraxial mesoderm.

MATERIALS AND METHODS

Animals

Mouse embryos were collected from $B_6D_2F_1$ matings and staged by considering noon of the plugging day as 0.5 dpc (day postcoitum). Both pigmented and albino *Xenopus laevis* females were used to collect the unfertilized eggs, and fertilization of eggs and manipulation of embryos were performed according to Moon and Christian (1989).

cDNA Library Construction and Yeast Two-Hybrid Screening

Head and forelimb buds of mouse embryos of 9.5 dpc were removed and the trunks were collected to prepare poly(A)$^+$ RNA. After random-primed cDNA was synthesized, *Eco*RI adaptors were added at the end of cDNAs and the resulting cDNAs were ligated into *Eco*RI-digested Hyb-ZAP λ DNA (Stratagene) and packaged. The titer of the primary cDNA library was 5×10^6 pfu and the average insert size was about 1.0 kb with over 85% insertion efficiency. The λ library was amplified and converted into plasmid form according to the manufacturer's protocol (Stratagene). A DNA fragment encoding the bHLH domain of mouse E47 protein (from aa 526 to aa 623) was fused to the GAL4 DNA binding domain in GAL4 DB plasmid (Stratagene). Five hundred micrograms of cDNA library plasmid and 50 μg of E47 bHLH bait plasmid were cotransformed into YRG2 yeast cells. A total of 7×10^6 independent transformants were screened by expression of the auxotropic marker and by lacZ expression. Sixty-four cDNAs containing either the bHLH or the HLH domain were isolated. These cDNAs represent 11 different bHLH (or HLH) genes, including 9 known genes and 2 novel ones (Table 1).

Molecular Biology and RNA Injection

A full-length mouse *pMesogenin1* cDNA sequence was determined from the cDNA clones generated by 5′ and 3′ RACE PCR. A DNA fragment encoding the bHLH domain of *Xenopus pMesogenin1* was amplified from *Xenopus* genomic DNA by PCR with degenerate primers derived from the consensus sequence of mouse *pMesogenin1, MesP1,* and *MesP2* bHLH domains. The primer sequences were 5′-GCC AGC GAG (A/C)GN GAG AA(A/G) CTN (A/C)GN ATG-3′ (forward primer) and 5′-(G/C)A(G/C) (A/G)GC NGA (G/C)AG GTG (G/C)CC (G/A)AT GTA NC(G/T) (G/A)AT-3′ (reverse primer). The full-length cDNA was also obtained by fusion of 5′ and 3′ RACE PCR products from *Xenopus* embryonic RNA (mixture of embryos from different stages ranging from blastula to tailbud). The coding sequences of both mouse and *Xenopus pMesogenins* were inserted into both CS2+ and CS2+MT vectors (gifts from Dr. David Turner) to generate DNA templates for capped RNA synthesis. DNA template for *VegT* was obtained from Dr. Mary Lou King (Zhang and King, 1996). Capped RNAs were synthesized using SP6 RNA polymerase and prepared as described previously (Moon and Christian, 1989). Normally, 0.5 to 4 ng *pMesogenin1* RNA or 1 to 2 ng *VegT* RNA was injected into embryos, as indicated in figure legends. Capped RNA was injected into the animal pole of both blastomeres of two-cell embryos for animal cap explant culture or into the marginal zone of either dorsal or ventral blastomeres of four-cell embryos for whole-mount *in situ* hybridization.

Animal Cap Explant Culture and RT-PCR

At stage 8, the animal caps were excised from the embryos injected with RNA and cultured until stage 10.5 or 12. RNA was isolated from 15 to 20 caps according to Chomczynski and Sacchi (1987). RNA was treated with DNase I to remove any residual genomic DNA contamination and cDNA was synthesized from 2 to 3 μg of total RNA by oligo(dT) priming. When whole embryos were used, two to three embryos were used to prepare RNA. One-tenth of the cDNA was used for each PCR including [^{32}P]dCTP. One-third of the reaction was analyzed on 5% nondenaturing acrylamide (29:1) gel in 1× TBE buffer. The RT-PCR primers for *EF1α, XMyoDa, XMyf-5, Xbra, Xwnt8, Mix.1, Chordin,* and *goosecoid* genes were synthesized as described in the *Xenopus* Resource Web site (http://vize222.zo.utexas.edu). The other PCR primers used in RT-PCR were as follows: *pMesogenin1,* 5′-GAT TCT GCA GGA GCT GAG GAC-3′ (forward) and 5′-GCA TGG CAG GGG TAC ACA GAC-3′ (reverse); *VegT,* 5′-CAA GTA AAT GTG AGA AAC CGT G-3′ (forward) and 5′-CAA ATA CAC ACA CAT TTC CCG A-3′ (reverse); *Eomesodermin,* 5′-GAT TCA GGG GTG TAT ACG GG-3′ (forward) and 5′-CAT GGC TGA GTG AGG ACG CC-3′ (reverse); *ESR4,* 5′-TCC CAA AAC TGA GAA GGC TGA TA-3′ (forward) and 5′-GTC TGG TTC TTG GGG CTT TGT TCC-3′ (reverse); *ESR5,* 5′-TGA AAA CAC ATG ATC CGA ATA AG-3′ (forward) and 5′-GAC AGT TCA CTC CCG TTG GAC-3′ (reverse); *Thylacine2,* 5′-CTT GCA TAC TAA TCA CGT CCA AC-3′ (forward) and 5′-AAA GGC ATA AAT ATT GTC TAC CGA C-3′ (reverse); and *Xmax2,* 5′-GTG GAA AGC GAC GAA GAC TC-3′ (forward) and 5′-CCG AGC TCG AGT AGT TGG AC-3′ (reverse).

Whole-Mount in Situ Hybridization and Histology

Whole-mount *in situ* hybridization of mouse embryos and *Xenopus* embryos follows the protocol described previously (Henrique *et al.,* 1995). For mouse and *Xenopus pMesogenin1* RNA *in situ,* either the 5′ or the 3′ end of the cDNA produced from RACE PCR was used to produce either digoxigenin (DIG)-labeled or fluorescein-labeled RNA probes. Both 5′ and 3′ probes produced identical staining patterns. DIG riboprobes for *MesP1, MesP2, Brachyury T, Tbx6, Paraxis, VegT, Xombi, XMyf-5, Xwnt-8, Xbra,* and *Chordin* were synthesized from the template DNAs as described previously (Burgess *et al.,* 1995; Chapman *et al.,* 1996; Christian *et al.,* 1991; Hopwood *et al.,* 1989, 1991; Lustig *et al.,* 1996; Saga *et al.,* 1996, 1997; Sasai *et al.,* 1994; Smith *et al.,* 1991; Zhang and King, 1996). Whole embryos or embryo explants were embedded in paraffin and the sections were stained with both hematoxylin and eosin as described previously (Kelly *et al.,* 1991).

RESULTS

Isolation of Novel bHLH Genes Expressed during Early Mouse Embryogenesis

bHLH class genes function in a variety of important transcriptional regulatory networks including skeletal myogenesis and neurogenesis (Dambly-Chaudiere and Vervoort, 1998; Kageyama and Nakanishi, 1997; Yun and Wold, 1996). A number of new bHLH genes have been isolated previously by two-hybrid interaction screening using E12 or *Daughterless* bHLH domains as the interaction bait from

TABLE 1
bHLH Genes Isolated from Mouse e9.5 Trunk cDNA Library by Yeast Two-Hybrid Screening

Gene	Number of clones
dHAND	7
eHAND	3
Id2	26
Id3 (bHLH462)	8
Paraxis	8
Mash-1	3
Math-1	1
MRF4	3
SEF-2	1
pMesogenin1 (novel)	1
T117 bHLH (novel)	3
Total number of cDNA clones	64

either mouse or chicken whole embryonic cDNA libraries (Buchberger *et al.*, 1998; Cserjesi *et al.*, 1995; Hollenberg *et al.*, 1995; Li *et al.*, 1995). In the present study we made two modifications designed to bias the outcome in favor of novel bHLH genes expressed along the developing vertebrate trunk. First, a new cDNA library was constructed from isolated e9.5 mouse embryo trunks, lacking the limbs and head. The intent was to enrich in favor of paraxial mesoderm and to include all of its major developmental stages as they are arrayed along the rostrocaudal axis to include mature patterned somites near the head to new unsegmented mesoderm in the tail bud. Second, we used the E47 bHLH domain as the protein interaction bait because it differed most strongly in sequence from the E12 and daughterless bHLH domains which had been used previously by other workers (Buchberger *et al.*, 1998; Cserjesi *et al.*, 1995; Henthorn *et al.*, 1990; Hollenberg *et al.*, 1995; Li *et al.*, 1995). The rationale was that the E47 bait might capture partners that pair preferentially with E47 compared with other E proteins that had already been used in prior screens. From a screening of 7×10^6 cDNA clones, we isolated 64 cDNA clones encoding bHLH or HLH domains. They represented 11 different genes including two novel ones (see Table 1).

pMesogenin1 Coding Sequences from Mouse and Frog

One of the two novel bHLH genes isolated from the screening is named *pMesogenin1* (*pMsgn1*), because of its expression pattern and its activities in mesoderm induction assays (see below). DNA sequencing and conceptual translation of a full-length cDNA revealed a candidate protein coding sequence of 188 amino acids in which the bHLH domain is located very close to the carboxyl terminus. Consistent with this, *in vitro*-translated protein synthesized from a full-length cDNA template behaved as a 19-kDa protein in SDS gel electrophoresis (Yoon and Wold, unpublished data). To facilitate a gain-of-function analysis for this gene, we next isolated a closely related gene from *X. laevis* by PCR from degenerate primers whose design was based on the mouse *pMesogenin1* and *MesP1/2* bHLH domain protein sequences (see below and Materials and Methods). The *Xenopus pMesogenin1* ORF consists of 173 amino acids. The deduced amino acid sequences for mouse and *Xenopus pMesogenin1* are compared in Fig. 1A. Sequence similarity is evident throughout, and there is a striking near-identity in the bHLH domains. A database search of GenBank using the full mouse *pMesogenin1* protein coding sequence identified members of the *MesP1/2* bHLH subgroup (Fig. 1C) as the most closely related mammalian genes (Saga *et al.*, 1996, 1997), although the similarity diminishes greatly outside the bHLH domain, as is typical of paralogous genes within the bHLH superfamily. In addition, the *Xenopus Mespo* protein coding sequence was found and proved to be very similar to mouse *pMesogenin1* (Joseph and Cassetta, 1999). Direct comparison showed that it is essentially identical to *Xenopus pMesogenin1*, and we provisionally conclude that they are from the same gene.

It appears very likely that the mouse and *Xenopus pMesogenins* are orthologous on the basis of three observations. First, *Xenopus* and mouse *pMesogenins* are more similar to each other (46% amino acid identity over the entire ORF and 81% identity in bHLH region) than is either one to murine *MesP1* and *MesP2* or to the known *MesP1* counterparts from chicken (*cMeso-1*) and *Xenopus* (*Thylacine1* and *2*) (from 62 to 53% identity in bHLH region) (Buchberger *et al.*, 1998; Sparrow *et al.*, 1998). Indeed, when the sequence comparison is made using only the non-bHLH domains of mouse and *Xenopus pMesogenin1*, there is no detectable similarity to the *MesP1/2* subgroup. The second reason for thinking that murine and *Xenopus pMesogenins* are orthologous with each other is that their overall primary sequence organization is shared between them but differs with other relatives. The *pMesogenin1* bHLH domains are positioned only a few residues from their carboxy termini, whereas in all *MesP1/2* family members the bHLH domain is located either in the middle or more toward the amino terminal of the protein sequences (Fig. 1C; Buchberger *et al.*, 1998; Saga *et al.*, 1996, 1997; Sparrow *et al.*, 1998). A dendrogram illustrating the protein sequence relatedness for mouse and *Xenopus* bHLH genes closest to *pMesogenin1* is shown in Fig. 1D. In this analysis, *pMesogenin1* from mouse and *Xenopus* are more closely related with each other than either is to any other gene known. Finally, as shown in the next section, the case for an orthologous relationship of mouse and *Xenopus pMesogenins* is made quite compelling by the fact that both mouse and *Xenopus pMesogenins* display identical activities in functional assays and by their remarkably similar RNA expression patterns in presomitic paraxial mesoderm, a pattern that is very clearly distinct from *MesP1/2*, *Thylacine 1/2*, and *cMeso-1*.

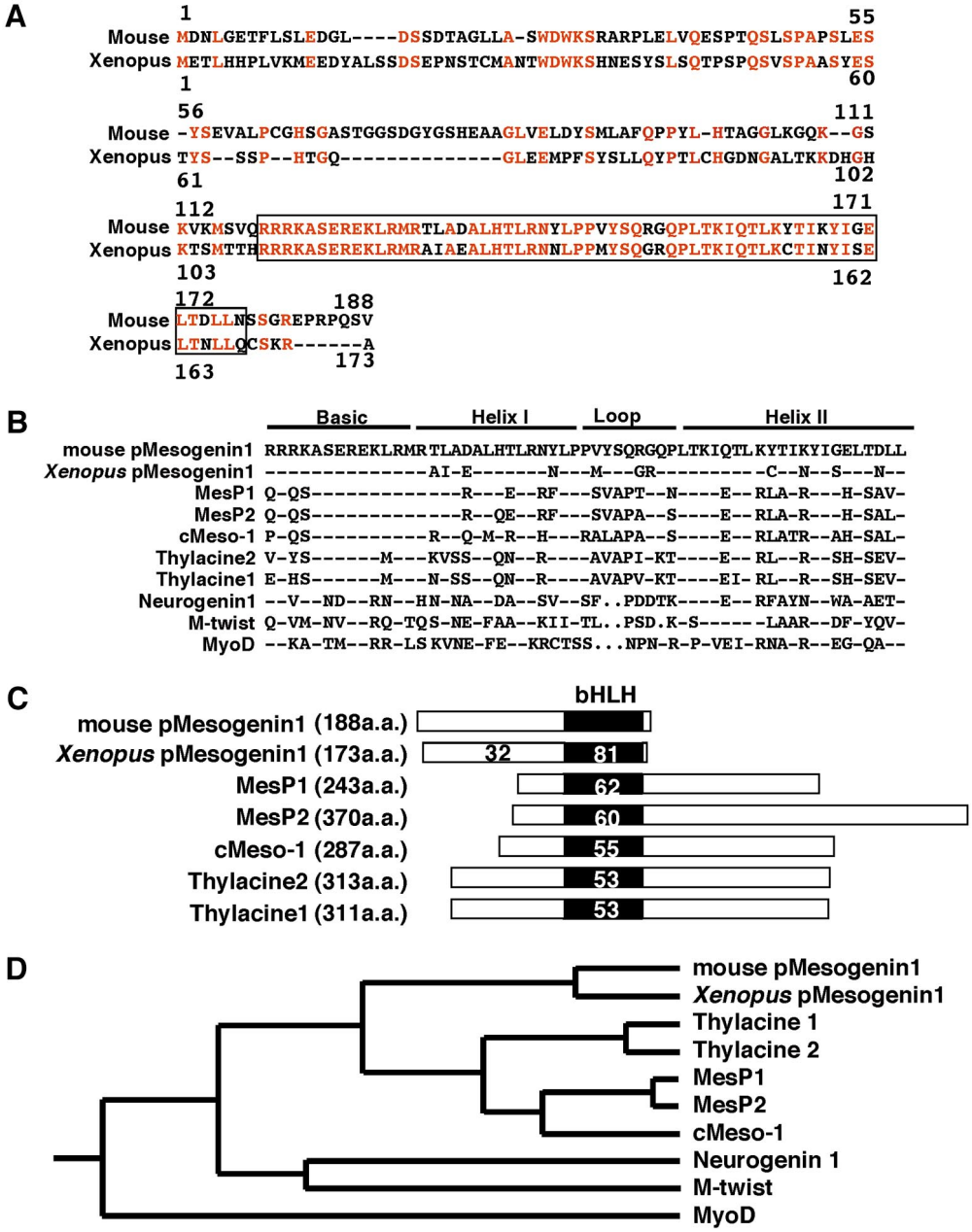

FIG. 1. *pMesogenin1* encodes a novel bHLH transcription factor. (A) Deduced amino acid sequences of *pMesogenin1* from both mouse and *Xenopus.* The sequences were aligned using the BESTFIT program in a GCG package. Identical amino acids are indicated as red letters. The bHLH domain is blocked. (B) Comparison of bHLH domain of pMesogenin1 to other closely related bHLH proteins in vertebrates. The peptide sequence of the bHLH domain of mouse pMesogenin1 was used to perform a BLAST search. The six top matched sequences were selected and aligned to each other using the CLUSTALW program. Sequences of Neurogenin1, M-Twist, and MyoD were also included in the alignment. Identical amino acids are indicated as a hyphen and gaps are indicated as a period. (C) Schematic diagram showing similarities among *pMesogenin1* and its related bHLH genes. The bHLH domain is colored black. Numbers on the boxed areas indicate the percentage of same amino acids in the domain compared to mouse *pMesogenin1.* (D) Phylogenetic dendrogram of pMesogenin1 and its related bHLH proteins. The peptide sequences of the bHLH domains were analyzed by the Kimura method for distance calculation and the resulting distance matrix data were processed by the UGPMA method in the NEIGHBOR program of the PHYLIP sequence analysis software package to obtain a tree dendrogram.

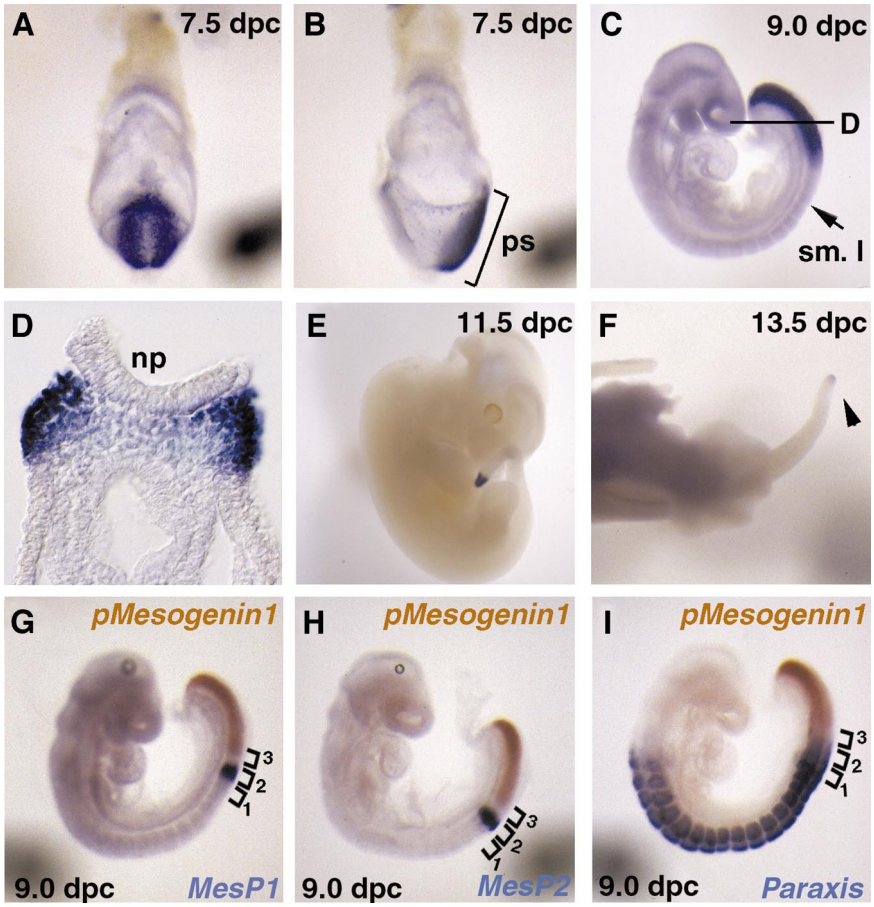

FIG. 2. *pMesogenin1* is expressed in a subdomain of the presomitic paraxial mesoderm and tailbud of the mouse embryo. (A–F) Expression of *pMesogenin1* in mouse embryos at 7.5 (A and B), 9.0 (C and D), 11.5 (E), and 13.5 dpc (F). (D) Transverse section of 9.0-dpc mouse embryo showing that *pMesogenin1* expression is exclusively localized in the paraxial mesoderm. np, neural plate. (G–I) Expression of *pMesogenin1* (brown color) and *MesP1*, *MesP2*, and *Paraxis* (purple color) is detected simultaneously in 9.0-dpc mouse embryos by two-color whole-mount *in situ* hybridization. The somitomeres 1 to 3 are marked by the brackets.

Comparative Expression of pMesogenin1 and MesP1/2

pMesogenin1 RNA expression during development was analyzed in detail by whole-mount *in situ* hybridization of both mouse and *Xenopus* embryos. In the mouse at 6.5 dpc, no RNA expression was detected (data not shown). In mouse embryos of 7.5 dpc, *pMesogenin1* expression is detected mainly in the posterior region of the embryo lateral to the primitive streak where presumptive progenitors of paraxial mesoderm reside (Figs. 2A and 2B). The expression is largely excluded from the midline of the primitive streak (Fig. 2A). No expression was detected in the anterior part of the embryo. Strong *pMesogenin1* expression was evident in the caudal presomitic mesoderm in the embryo at 9.0 dpc (Figs. 2C and 2D). The rostral boundary of the *pMesogenin1* expression domain is about two somite lengths (two somitomeres or somitomere 1 and 2, also see Fig. 8A) distant from the posterior boundary of the most newly formed somite (somite I). Within the expression domain of *pMesogenin1*, some embryos showed detectably weaker staining in the most rostral positive somitomere (somitomere 3), and we speculate that this reflects an intermediate state of expression in which rapid decay of *pMesogenin1* RNA occurs as somitomere 3 is transformed into somitomere 2. Later, in embryos of 11.5 dpc, the primitive streak has completely regressed, and *pMesogenin1* RNA is observed exclusively in the tailbud (Fig. 2E). This expression remains in the tailbud until 13.5 dpc (Fig. 2F) and begins to disappear between 13.5 and 14.5 dpc when the tailbud loses its potential to provide paraxial mesoderm cells (Tam and Tan, 1992). The bHLH genes most closely related to *pMesogenin1*, *MesP1* and *MesP2*, are also expressed in the presomitic mesoderm (Saga *et al.*, 1996, 1997). Using two-color whole-mount *in situ* hybridization,

we compared the expression domains of *MesP1/2* and *pMesogenin1* more precisely. *MesP1/2* RNA expression is visible in somitomere 2 (Figs. 2G and 2H; Saga *et al.*, 1997) and in rare embryos is observed in both somitomeres 2 and 1 (Yoon and Wold, unpublished data; Buchberger *et al.*, 1998). Thus, it appears that *pMesogenin1* and *MesP1/2* expressions are mutually exclusive. Expression of *pMesogenin1* was also compared with that of another bHLH gene, *Paraxis*, which is expressed in the most rostral presomitic mesoderm as well as in some subdomains of more differentiated somites of midgestation mouse embryos (Burgess *et al.*, 1995). Expression of *Paraxis* and *pMesogenin1* also displays little or no overlap. The caudal boundary for *Paraxis* expression appears to meet *pMesogenin1* expression at the junction of somitomeres 2 and 3. *Paraxis* expression does, however, appear to overlap fully with *MesP1/2* in the PSM (Figs. 2I and 8A).

We next determined the pattern of *pMesogenin1* RNA expression during *Xenopus* development, initially using RT-PCR (Fig. 3A). Expression was first detected at gastrulation. *pMesogenin1* was then observed throughout development until the tadpole stage. Even very high sensitivity RT-PCR assays detected no *pMesogenin1* signal from unfertilized eggs or from embryos at stages before midblastula transition, suggesting that *pMesogenin1* expression in *Xenopus* is entirely zygotic (Fig. 3A). Whole-mount *in situ* hybridization experiments were consistent with the RT-PCR survey and clarified spatial domains of expression. *pMesogenin1* RNA is predominantly localized in ventrolateral mesoderm but is absent from dorsal mesoderm in gastrulae (Figs. 3B and 3C). In tailbud stage embryos, *pMesogenin1* expression is still detected and is localized to the most caudal (unsegmented) paraxial mesoderm. At the tadpole stage, expression remains in the tailbud (Figs. 3D and 3E). Where the developmental stages tested were similar, the patterns of *Xenopus pMesogenin1* expression agree with those of *Mespo* expression (Joseph and Cassetta, 1999). The analogous expression patterns of *pMesogenin1* in mouse and *Xenopus* embryos suggest that they might play a similar role in paraxial mesoderm formation in both organisms.

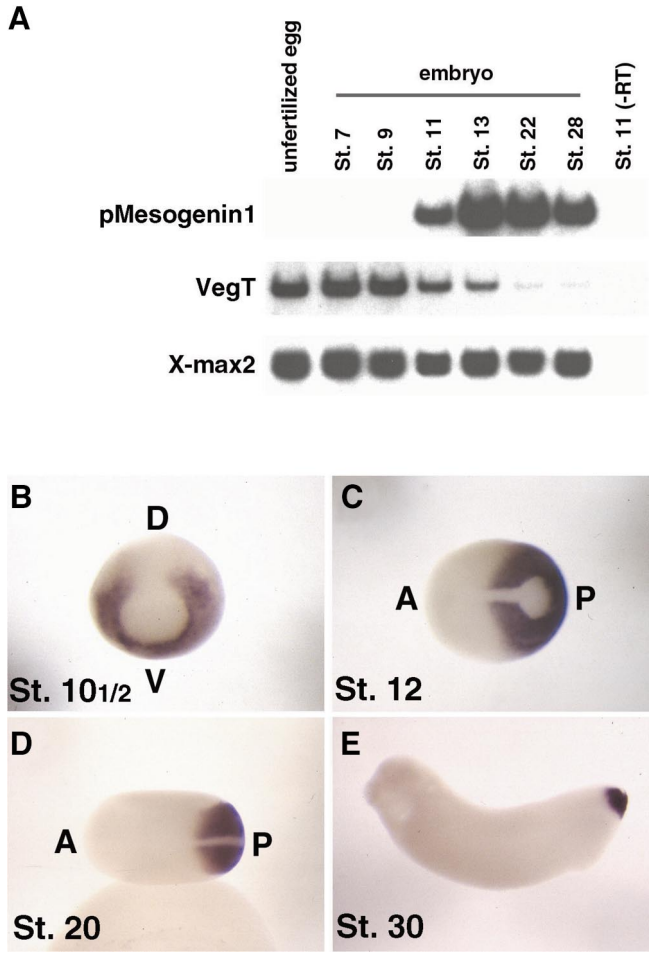

FIG. 3. *pMesogenin1* is zygotically expressed in presumptive mesoderm of gastrulae and tailbud region in *Xenopus* embryos. (A) RT-PCR analysis of *pMesogenin1* expression shows that *pMesogenin1* is zygotically expressed and developmentally regulated during *Xenopus* embryogenesis. T-box transcription factor *VegT*, on the other hand, is expressed both maternally and zygotically (Zhang and King, 1996). *X-max2* gene expression (King *et al.*, 1993) was also monitored as a control for RT-PCR. (B–E) Whole-mount *in situ* analysis of *pMesogenin1* expression during *Xenopus* embryogenesis. During gastrulation, *pMesogenin1* expression was detected in ventrolateral mesoderm. After gastrulation, *pMesogenin1* is expressed in the tailbud (presomitic mesoderm) region until early tadpole stage. Abbreviations: D, dorsal; V, ventral; A, anterior; and P, posterior.

pMesogenin1 Can Induce Presomitic Paraxial Mesodermal Phenotypes

Based on the prominent expression of *pMesogenin1* in early mesoderm and its absence from ectodermal or endodermal germ layers, we asked whether its ectopic expression could induce a mesodermal phenotype in presumptive ectoderm. *In vitro*-synthesized *pMesogenin1* RNA samples from either mouse or *Xenopus* gene templates were injected into the animal pole of both blastomeres of two-cell stage embryos. Animal caps were explanted at blastula stage and cultured until companion wild-type embryos reached the gastrula stage. Pooled caps were then assayed by RT-PCR for expression of a battery of molecular markers of mesoderm and endoderm. The results were very similar for both mouse and frog *pMesogenin1* injections. As might have been expected, expression of *Mix1*, a molecular marker for endoderm, was never detected in *pMesogenin1*-injected caps (Fig. 4A). Several well-studied molecular markers of ventrolateral mesoderm such as *XMyoD* (Hopwood *et al.*, 1989), *XMyf-5* (Hopwood *et al.*, 1991), and *Xwnt-8* (Christian *et al.*, 1991) were reproducibly induced by both mouse and *Xenopus pMesogenin1* (Fig. 4A).

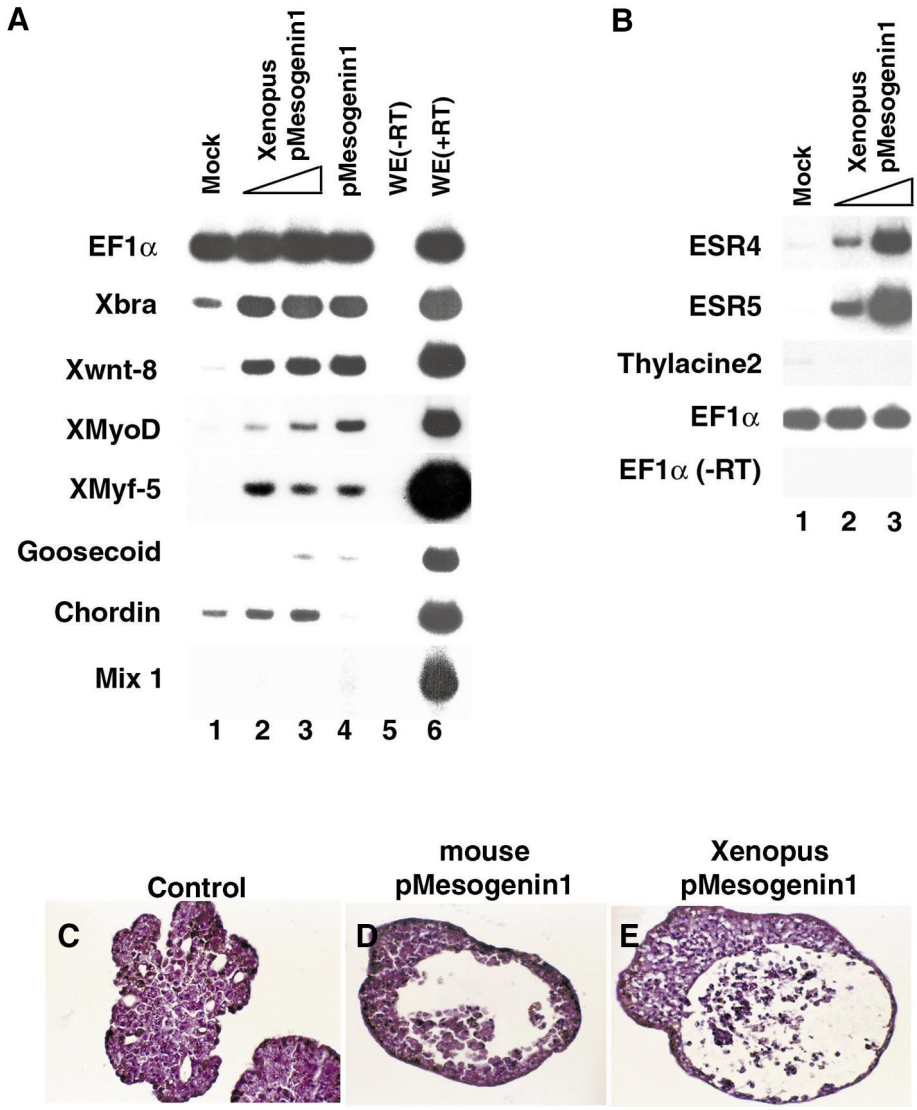

FIG. 4. *pMesogenin1* induces presomitic paraxial mesoderm markers in animal cap explants. (A and B) RT-PCR analysis of mesoderm marker gene expression in animal cap explants injected with either mouse or *Xenopus pMesogenin1* RNA. Water (Mock) or *Xenopus* (0.5 and 2 ng per embryo) or mouse *pMesogenin1* RNA (2 ng per embryo) was injected into the animal pole of both blastomeres of two-cell stage embryos, which were explanted at stage 8 and cultured until stage 10.5 (A) or stage 12 (B). Expression of a number of marker genes was analyzed by RT-PCR. At least three independent experiments were done and produced the same results. Data from one experiment are shown here. (C–E) Overexpressed *pMesogenin1* induced ventrolateral phenotypes in animal cap explants cultured until the time equivalent of stage 35 to 36. The culture explants were paraffin embedded, sectioned, and stained with hematoxylin and eosin. Explants injected with *pMesogenin1* (2 ng per embryo) develop a cavity filled with mesenchymal cells, which is a typical phenotype for lateral ventral mesoderm induction.

These results are consistent with a potential role for *pMesogenin1* in normally regulating these genes *in vivo*, since the expression of *pMesogenin1* in intact *Xenopus* embryos overlaps with the expression of *XMyoD*, *XMyf-5*, and *Xwnt-8*. The panmesodermal marker *Xbra* (Smith *et al.*, 1991) was efficiently induced by *pMesogenin1*.

In contrast to markers of ventrolateral mesoderm, molecular markers of dorsal mesoderm or Spemann's organizer were not comparably induced by *pMesogenin1* in the animal cap assay (Fig. 4A). For example, *goosecoid* (Cho *et al.*, 1991) is a marker specific for the organizer (future axial mesoderm that gives rise to the notochord), and it was expressed very weakly in some experiments and not at all in others. Another dorsal mesoderm marker, *Chordin* (Sasai *et al.*, 1994), was never detectably induced in animal caps injected with mouse *pMesogenin1* RNA and was expressed

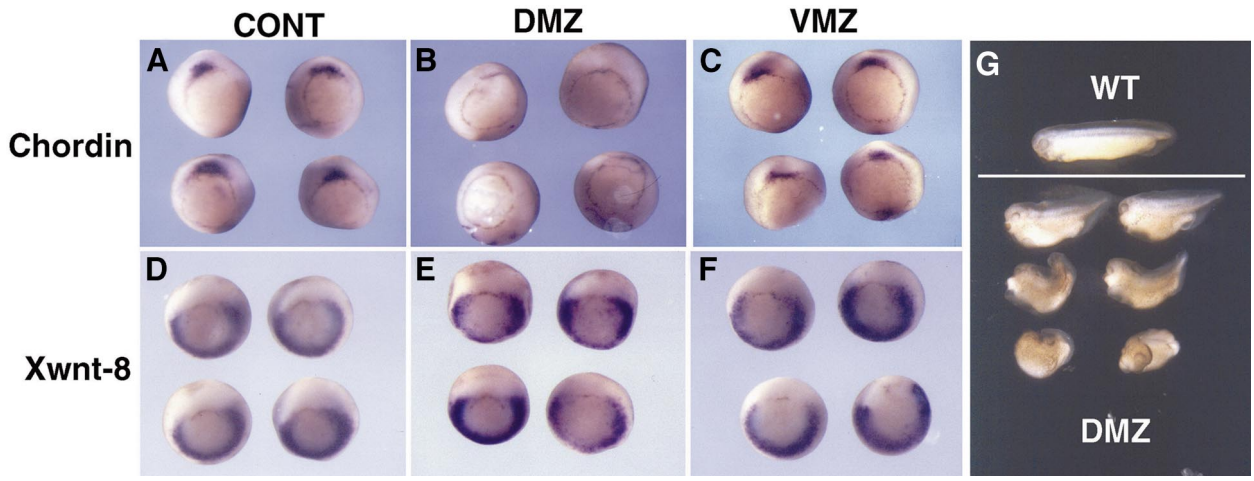

FIG. 5. Ectopically expressed *pMesogenin1* suppresses dorsal mesoderm formation. *pMesogenin1* RNA (4 ng per embryo) was injected into either the dorsal (DMZ) or the ventral (VMZ) marginal zone of four-cell stage blastomeres, and expression of the dorsal marker *Chordin* (A, B, and C) and ventrolateral mesodermal marker *Xwnt-8* (D, E, and F) was analyzed by whole-mount *in situ* hybridization. (G) Morphological defects in the tadpoles injected in the DMZ of four-cell stage embryos with *pMesogenin1*. Tadpoles showing more severe defects are arranged from top to bottom. *pMesogenin1* caused a failure of axis extension, probably due to the defect in dorsal structure formation.

only marginally in *Xenopus pMesogenin1* RNA-injected caps.

In late gastrula stage animal cap explants, paraxial or somitic mesoderm-specific markers such as *ESR4* and *ESR5* (Jen *et al.*, 1999) were also significantly induced by *pMesogenin1* (Fig. 4B). Finally, we assayed for expression of *Thylacine2*, because it is expressed specifically in paraxial mesoderm at later times (in somitomeres) after native *pMesogenin1* expression is shut down in the intact embryos. *Thylacine2* has been shown to act in regulation of proper somitogenesis and segmentation (Sparrow *et al.*, 1998). No expression of *Thylacine2* was induced in the cap assay (Fig. 4B).

Following more prolonged culture, animal cap explants injected with *pMesogenin1* RNA developed into distinctive round balls. In cross sections histological staining showed a cavity inside partially filled with mesenchymal cells (Figs. 4D and 4E). This phenotype is markedly different from that of control caps (Fig. 4C) but is very similar to the phenotype that was previously associated with induction of ventrolateral mesoderm (Cunliffe and Smith, 1994), including ventrolateral mesoderm induced by *Xwnt-8* in the animal cap assay (Christian and Moon, 1993). Consistent with the molecular marker analysis at an earlier developmental time, no elongated explants or notochord-like structures, typical of dorsal mesoderm induction, were observed (Cunliffe and Smith, 1994). Taken together, the results from the animal cap experiments suggest that both *Xenopus* and mouse *pMesogenin1* can induce a ventral/lateral mesoderm cellular phenotype in the context of the presumptive ectoderm of animal caps, but that it does not induce dorsal mesoderm or endoderm phenotypes.

pMesogenin1 Can Disrupt Formation of Normal Dorsal Mesoderm

To further explore *pMesogenin1* regulatory capacities, *pMesogenin1* RNA was injected into the marginal zone of either dorsal or ventral blastomeres of four-cell stage embryos. At stage 11, expression of the dorsal marker *Chordin* was greatly reduced or abolished entirely in dorsally injected embryos (Fig. 5B). In contrast, normal *Chordin* expression was observed in both uninjected control embryos and embryos injected with *pMesogenin1* RNA in the ventral marginal zone (Figs. 5A and 5C). Additionally, embryos dorsally injected showed a significant morphological defect at the tadpole stage (Fig. 5G). The injected embryos showed a truncated body axis, indicating deficits in either dorsal axial or paraxial extension (Fig. 5G). Histological examination of transverse sections from severely affected embryos at stage 35 showed failure of proper notochord and neural tube formation (data not shown). The strong notochord and neural tube phenotypes, however, were not observed in more mildly foreshortened embryos in which the only effect we detected was on overall body extension. These results extend the animal cap results in which dorsal mesodermal marker genes were not induced by showing that ectopic *pMesogenin1* can actively suppress formation of dorsal mesodermal derivatives in the context of the whole embryo. However, in contrast to the animal cap assay, in this whole-embryo assay expression of the ventrolateral mesodermal markers *Xwnt-8, XMyoD,* and *XMyf-5* was not significantly elevated at stage 11 (Figs. 5D–5F; data not shown). A possible explanation is that the domain of future dorsal mesoderm of whole embryos represents a

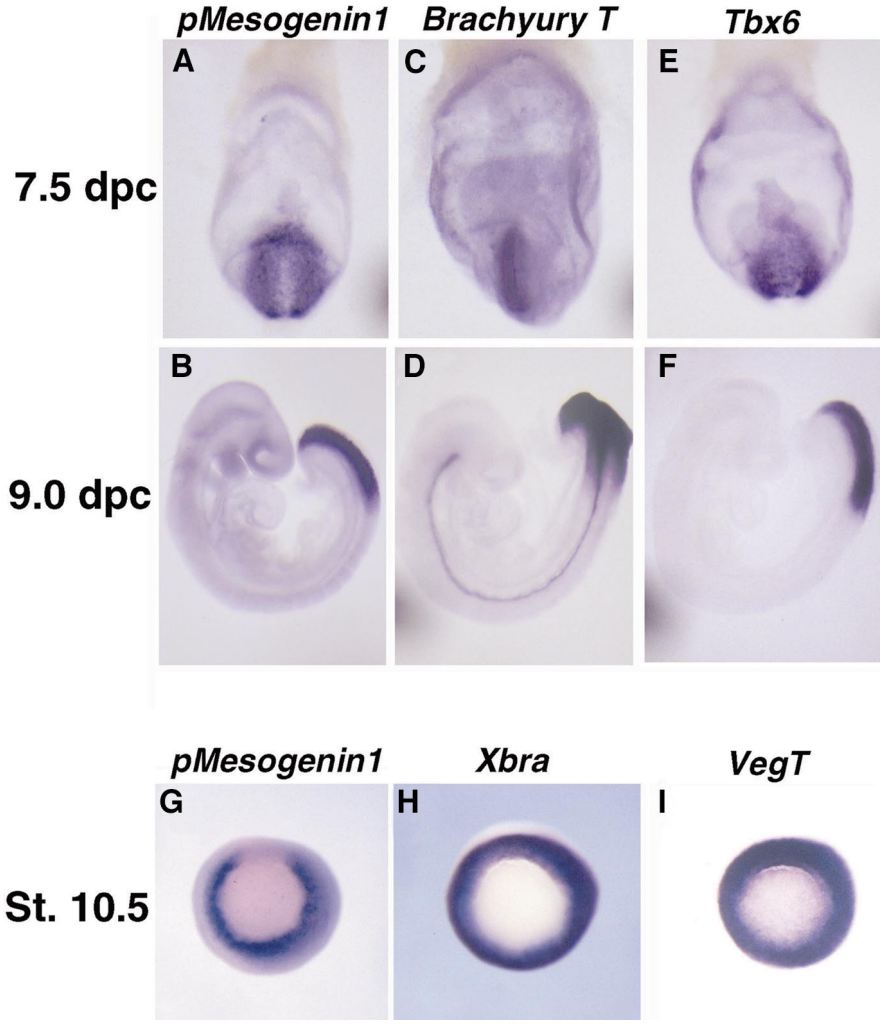

FIG. 6. Comparative analysis of expression of *pMesogenin1* and T-box transcription factor genes in mouse and *Xenopus* embryos. (A–F) *pMesogenin1* (A and B), *Brachyury T* (C and D), and *Tbx6* (E and F) expression was examined by whole-mount *in situ* hybridization of mouse embryos at 7.5 (A, C, and E) and 9.0 dpc (B, D, and F). (G–I) *pMesogenin1* (G), *Xbra* (H), and *VegT* (I) expression was monitored in *Xenopus* embryos at gastrulation stages.

more developmentally stringent environment than do animal cap explants lacking the influences of endoderm and of normal mesoderm formation.

pMesogenin1 and Mesodermal T-Box Transcription Factors

In mouse and frog combined, four T-box class transcription factors are recognized as functionally important regulators of mesoderm development: *VegT* (Horb and Thomsen, 1997; Lustig *et al.*, 1996; Stennard *et al.*, 1996; Zhang and King, 1996) and *Eomesodermin* (Ryan *et al.*, 1996) in *Xenopus*, *Xbra* in *Xenopus* (*Brachyury T* in mouse) (Herrmann *et al.*, 1990; Smith *et al.*, 1991), and *Tbx6* in mouse (Chapman *et al.*, 1996). These genes are expressed in presomitic paraxial mesoderm of mouse and *Xenopus* embryos but most of these T-box regulators also have additional domains of expression. We therefore compared more closely expression of *Brachyury T*, *Tbx6*, and *VegT* with that of *pMesogenin1* in mouse and *Xenopus* (Fig. 6). In the mouse at 7.5 dpc, *Brachyury T* expression was detected mainly in the primitive streak as described previously (Fig. 6C). The streak at this time is not a domain of detectable *Tbx6* or *pMesogenin1* expression; their expression is localized laterally relative to the streak where nascent paraxial mesoderm progenitors are thought to be located (Figs. 6A and 6E) (Lawson and Pedersen, 1992; Schoenwolf, 1999; Tam and Beddington, 1992). In mouse embryos at 9.0 dpc, *Brachyury T* expression is detected in the caudal presomitic paraxial mesoderm as well as in the notochord (Fig. 6D), while

pMesogenin1 and *Tbx6* expression is restricted to the presomitic mesoderm and is absent from the notochord (Figs. 6B and 6F). *Brachyury T, Tbx6,* and *pMesogenin1* RNAs also begin to disappear simultaneously from the tailbud between 13.5 and 14.5 dpc (Fig. 2F; data not shown) when somite formation has ceased and the tailbud loses its activity as a paraxial mesoderm producer (Tam and Tan, 1992). Thus, at all stages examined, the expressions of *Tbx6* and *pMesogenin1* in mouse embryos are identical and are restricted to paraxial mesoderm or its putative immediate progenitors, while *Brachyury T* expression overlaps in paraxial mesoderm but is also expressed earlier and in axial mesoderm (notochord).

A similar comparison was made of *Xbra, VegT,* and *pMesogenin1* expression in frog embryos. *VegT* and *pMesogenin1* are both expressed in ventrolateral mesoderm (future paraxial mesoderm) during gastrulation and in the tailbud at later stages (Figs. 3, 6G, and 6I; Zhang and King, 1996), but the picture in the axial/dorsal mesoderm differed from that in the mouse with respect to *VegT*. Stage 10 *Xenopus* embryos show this clearly. As expected, *Xbra* expression was detected in the entire presumptive mesoderm, including dorsal mesoderm of the future notochord (Fig. 6H). *VegT* is quite closely related to mouse *Tbx6*, although it is unclear whether they are orthologous. *VegT* RNA was detected in all presumptive mesoderm, including the future notochord (very similar to *Xbra*) as shown in Fig. 6I. This is a clear difference with mouse *Tbx6* in which there is no detectable *Tbx6* expression in notochord. *pMesogenin1* RNA was conspicuously absent from dorsal mesoderm.

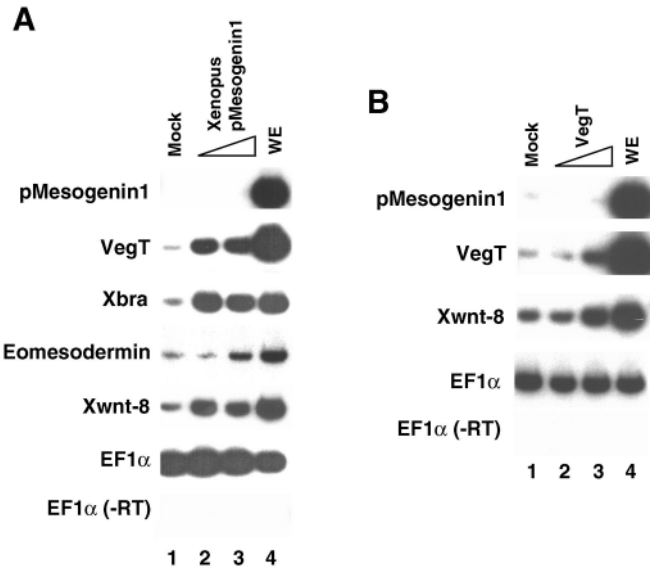

FIG. 7. Interactions between *pMesogenin1* and T-box genes. (A) RT-PCR analysis of T-box gene expression in animal cap explants injected with *Xenopus pMesogenin1* RNA (0.5 and 2 ng per embryo). The animal cap explants were harvested at stage 11 (midgastrulation). (A) *pMesogenin1* induced *Xbra* and *VegT* expression readily and *Eomesodermin* expression weakly. *pMesogenin1*, however, failed to induce accumulation of endogenous *pMesogenin1* RNA. (B) *VegT* failed to induce *pMesogenin1*. RT-PCR analysis of *pMesogenin1* expression in the stage 11 animal cap explants injected with *VegT* RNA (1 and 2 ng per embryo) showed no induction of *pMesogenin1* expression, but efficient induction of *VegT* itself and *Xwnt-8*. The data shown are from one of three independent experiments which produced essentially identical results.

pMesogenin1 Can Induce Expression of T-Box Transcription Factors

The overlap of *Xbra* (or *Brachyury T*), *VegT, Tbx6,* and *pMesogenin1* expression in ventrolateral mesoderm or paraxial mesoderm of mouse and *Xenopus* embryos raises the possibility that they might cross-regulate each other, either directly or indirectly, during paraxial mesoderm formation. We therefore asked whether *Xbra, VegT,* and another T-box gene, *Eomesodermin,* could be induced by *pMesogenin1* in the animal cap assay (Fig. 7). In *pMesogenin1*-RNA-injected animal cap explants there was significant induction of both *VegT* and *Xbra* and relatively weak induction of *Eomesodermin* (Fig. 7A). The converse, however, was not true as *VegT* RNA injection did not induce detectable expression from the endogenous *pMesogenin1* gene (Fig. 7B). With respect to autoregulation, *pMesogenin1* and *VegT* also differed. Injection of *pMesogenin1* RNA did not induce endogenous *pMesogenin1* expression while injection of *VegT* RNA did induce expression of endogenous *VegT,* as reported previously (Fig. 7B; Zhang and King, 1996). These data show that *pMesogenin1* has the capacity to induce expression of T-box transcription factors such as *Xbra, VegT,* and *Eomesodermin,* which may correspond to a regulatory capacity operating in future ventrolateral mesoderm of the intact embryo.

DISCUSSION

Results of functional assays reported here led to a central conclusion that *pMesogenin1* has the regulatory capacity to specify ventrolateral (including future paraxial), but not dorsal (future axial), mesoderm phenotypes, which is consistent with its domain of expression (Figs. 4, 5, and 6). This distinguishes *pMesogenin1* from other known transcriptional regulators of mesoderm that induce panmesodermal phenotypes. A related conclusion is that *pMesogenin1* has the regulatory capacity to disrupt normal development of axial mesoderm. The relationship of this regulatory capacity to the activities of specific induced target genes such as *Xwnt-8* is discussed below. Another major conclusion was that *pMesogenin1,* like its closest relatives, *MesP1/2* (*Thylacine1/2* in *Xenopus*), is an upstream regulator of at least some elements of the *Notch/Delta* signaling appara-

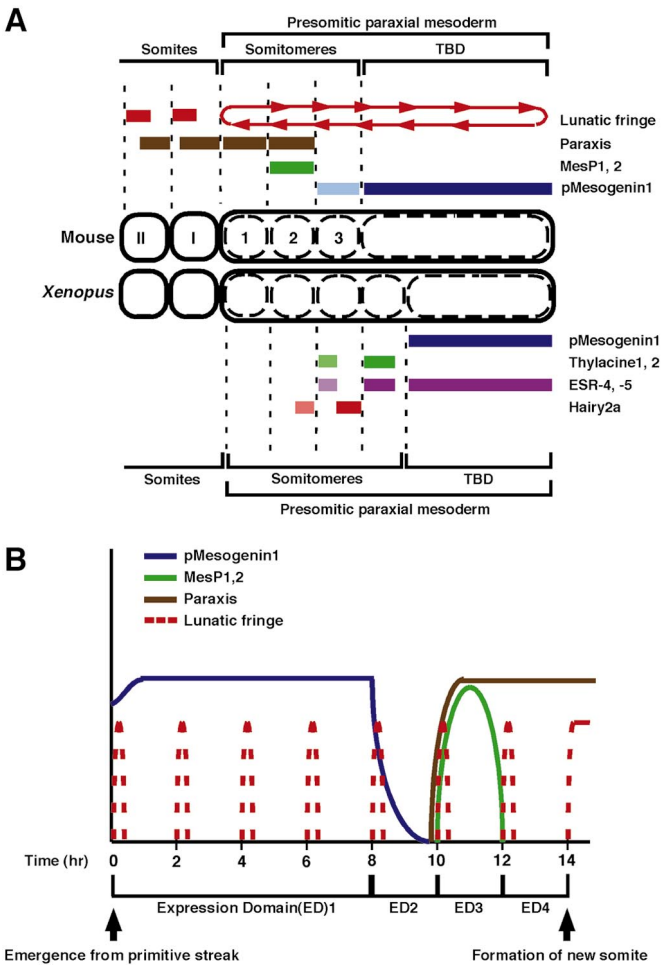

FIG. 8. Summary model of spatial and temporal patterns of expression for *pMesogenin1/MesP1* and additional pertinent of paraxial mesoderm formation and segmentation. (A) Summary model of spatial expression in presomitic paraxial mesoderm of the mouse (top) and *Xenopus* (bottom). Gene expression domains in presomitic paraxial mesoderm of mouse at ~9.0 dpc are taken from this study and from Barnes *et al.* (1997), Buchberger *et al.* (1998), Burgess *et al.* (1995), Forsberg *et al.* (1998), Sosic *et al.* (1997) and McGrew *et al.* (1998). The *MesP1/2* expression domain is marked as somitomere 2 (see text for further detail), and a similar expression pattern has been reported for *cMeso-1* in chicken embryos (Buchberger *et al.*, 1998). *Paraxis* expression in our study agreed with that of prior studies (Barnes *et al.*, 1997; Burgess *et al.*, 1995). Mouse *Lunatic fringe* is shown as a representative of the oscillating class of genes (Forsberg *et al.*, 1998; McGrew *et al.*, 1998; Palmeirim *et al.*, 1997). They oscillate with a period equal to that of somite formation (at this time in the mouse ~2 h per somite cycle) and the oscillating character is indicated by the arrowed oval in the PSM. It is not yet clear how similar oscillating patterns are for murine *Lunatic fringe* and *Hes1*. In *Xenopus* embryos, presomitic paraxial mesoderm consists of four somitomeres and the tailbud domain (TBD), which were defined mainly based on expression patterns of marker genes (Jen *et al.*, 1999). For simplicity, we show no numbering scheme here for *Xenopus* somitomeres. Jen *et al.* (1999) use a numbering system that labels the most caudal somitomere of the known four as somitomere 1, with numbers increasing to the most rostral somitomere (No. 4). The *Xenopus pMesogenin1* (*Mespo*), *Thylacine1/2*, and *ESR4/5* expression domains were determined comparing patterns obtained for each of the individual hybridization probes in embryos of the same stages (Yoon and Wold, unpublished data). The overlap (or lack thereof) for these domains in *Xenopus* is, therefore, somewhat uncertain at the boundaries. For the model we draw on the analogy with the mouse two-color data in which the paralogs do not overlap. (B) Time course of gene expression for a PSM cell that exits from the mouse primitive streak at ~9.0 dpc. Expression domain (ED) 1 corresponds to TBD in A, ED2 to somitomere 3, ED3 to somitomere 2, and ED4 to somitomere 1. The periodicity for each somite formation in mouse embryo is approximately 2 h. The time and precise number of somitic cycles from the start to the boundary with the first new somite in this model are illustrated as 7, but the elapsed time in the tailbud domain shown here as 4 cycles is arbitrary. In the chicken, this number is better determined and 12 cycles precede the first somite at a comparable developmental stage (Palmeirim *et al.*, 1997). Note also that the shape of the expression profile for *Lunatic fringe* within each cycle is also arbitrary.

tus, which is needed for proper segmentation and somitogenesis (Fig. 4B; Buchberger *et al.*, 1998; Burgess *et al.*, 1996; Saga *et al.*, 1997; Sparrow *et al.*, 1998; Jen *et al.*, 1999). We also found that the spatial domains of *pMesogenin1* expression are entirely consistent with results from the functional assays (Figs. 2 and 3). By using comparative expression data from mouse and frog, coupled with the improved resolution afforded by two-color expression analyses for key pairs of mouse genes, we were able to define three distinct dynamic domains of bHLH gene expression within the presomitic paraxial mesoderm. These data are incorporated in a comparative spatial model (Fig. 8A) and a summary temporal model (Fig. 8B) as discussed below.

Two Forms of Dynamic Prepatterning of Presomitic Mesoderm

Presomitic paraxial mesoderm superficially appears to be a homogeneous block of tissue, but this impression is misleading. High-resolution ultrastructural studies (Jacobson, 1993) and, especially, gene expression patterns are revealing that the presomitic paraxial mesoderm is elaborately prepatterned. This prepatterning is highly dynamic with waves of specific gene expression occurring in the spatiotemporal domain that immediately precedes birth of the newest somite (Gossler and de Angelis, 1998; Tam and Trainor, 1994).

The dynamic quality of PSM gene expression domains is of two distinct forms. First, there are domains that change rapidly and continuously as part of the moving wave of new somite formation (*MesP1/2*, caudal *Paraxis*, and rostral *pMesogenin1* in the mouse; *Thylacine1/2*, rostral *pMesogenin1*, and *ESR4/5* in *Xenopus*). A useful way to visualize this is to compare the composite gene expression pattern for

these genes illustrated at a single developmental time point (Fig. 8A) with a time domain model of expression for the same gene set (Fig. 8B). The latter is the deduced temporal expression pattern for each gene during the life of a single cell of the mouse PSM, beginning with that cell's emergence from the primitive streak (shown here for a cell emerging around 9.0 dpc). In the life of this cell, *pMesogenin1* has come on while the cell is part of the earliest presumptive mesoderm during gastrulation or possibly in immediate progenitors. *pMesogenin1* expression remains high and apparently uninterrupted throughout the time the cell is part of presomitomeric PSM (expression domain 1 in Fig. 8B). In the spatial domain, the cell in question would appear to be at an increasingly rostral position in the PSM due to addition of new cells behind it (caudally) and the advance of new somite formation ahead of it (rostrally). The second distinct expression state begins many hours later and is identified by cessation of *pMesogenin1* expression. There follows a short time (and space) in which there is no detectable *MesP1/2* or *pMesogenin1* RNA (expression domain 2 in Fig. 8B). This expression domain is, at most, one somitomere in width, which corresponds to about 2 h in time. This is also the time and spatial domain in which *Paraxis* expression begins. *Paraxis* is another bHLH regulator that is needed for somite epithelialization in the mouse (Burgess *et al.*, 1996), but it does not have a known ortholog in *Xenopus.* The third distinct expression state is defined by *MesP1/2* expression, the continued presence of *Paraxis* RNA, and no detectable *pMesogenin1* (expression domain 3). In the majority of mouse embryos, the implied duration of *MesP1/2* expression is less than 2 h, corresponding to a stripe of about one somite in width. This stripe appears to correspond to somitomere 2, as indicated in the model, although in a minority of embryos we observed two stripes of *MesP1/2* expression with the rostral one being weaker. We think these latter embryos are specimens caught in the midst of a transition in somitomere identity from 2 to 1 (Yoon and Wold, unpublished data; Buchberger *et al.*, 1998). The rostral boundary of the *MesP1/2* stripe appears to be approximately one somitomere distant from the border with the newest somite (Figs. 2 and 8A).

Detailed examination of *pMesogenin1* RNA at multiple developmental stages in *Xenopus* gave results strikingly similar to those in the mouse and this comparison led us to similar overall views for both organisms, and a model for the analogous set of events in *Xenopus* is shown (Fig. 8). We did not achieve as much resolution in *Xenopus* as in the mouse because of technical difficulties in obtaining similarly informative two-color *in situ* data. However, measurements with individual hybridization probes were robust and the results were consistent with *pMesogenin1* being expressed until *Thylacine1/2* comes on in somitomeres and we suggest this as a provisional model. Interestingly, Jen *et al.* (1999) showed that *ESR4/5* are expressed throughout the tailbud domain (the domain of *pMesogenin1*) and also in somitomeres where they overlap *Thylacine1/2* in the rostral halves. As we found that ectopic expression of *pMesogenin1* activates *ESR4/5* in animal cap assays, it seems possible that *ESR4/5* are targets (direct or indirect) of the *Thylacine/pMesogenin1* subgroup of bHLH regulators. It is not yet clear whether the mouse has genes orthologous to *ESR4/5.*

Oscillating Gene Expression in Presomitic Paraxial Mesoderm

A second and different form of dynamic prepatterning in the presomitic paraxial mesoderm is represented most clearly by expression of the *cHairy1,* a bHLH regulator of the *hairy* (WRPW) class in the chicken, and by expression of *Lunatic fringe* in the chicken and the mouse (Forsberg *et al.*, 1998; McGrew *et al.*, 1998; Palmeirim *et al.*, 1997). Their expression oscillates multiple times during the life of a single cell of the PSM (Fig. 8B; del Barco Barrantes *et al.*, 1998; Evrard *et al.*, 1998; Forsberg *et al.*, 1998; McGrew *et al.*, 1998; Zhang and Gridley, 1998). These multiple oscillations differ markedly from genes such as *pMesogenin1* and *MesP1/2* which have only a single continuous period of expression in the life of any given cell and its progeny (Fig. 8B). RNA-level oscillation of these genes has the periodicity of somite formation and is an autonomous property of the presomitic paraxial mesoderm which does not depend significantly on signals from adjacent tissues (Jiang *et al.*, 1998; Palmeirim *et al.*, 1997). The implication is that these periodically oscillating genes reflect the existence of a molecular clock and this clock is postulated to be intimately involved in regulating somitogenesis and segmentation.

The oscillating genes discovered thus far in mammals and birds are in molecular pathways associated with the *Notch/Delta* signaling system. Components of the *Notch/Delta* pathway have been knocked out in the mouse, and they disrupt somitogenesis and segmentation (Conlon *et al.*, 1995; deAngelis *et al.*, 1997; del Barco Barrantes *et al.*, 1998; Evrard *et al.*, 1998; Kusumi *et al.*, 1998; Swiatek *et al.*, 1994; Zhang and Gridley, 1998). Similarly, in *Xenopus,* Kintner and colleagues have used dominant negative regulators and gain-of-function assays to make a strong case that the *Notch/Delta* signaling pathway is a key modulator of segmentation and somitogenesis, including *ESR4/5,* which are immediately relevant to this work (Jen *et al.*, 1997, 1999; Sparrow *et al.*, 1998), although it has not yet been shown that any transcripts in *Xenopus* oscillate periodically in the manner of *cHairy1* or *Lunatic fringe.*

What relationship, if any, exists between the somitic clock and the genes of the *pMesogenin1* subfamily of bHLH regulators? Three lines of evidence suggest to us that there may be a functional connection between them. First, *ESR4/5* have been shown to be members of a novel branch of the *hairy* family of regulators in *Xenopus* that are part of the *Notch/Delta* signaling pathway in the presomitic paraxial mesoderm of the frog (Jen *et al.*, 1999), and we showed here that they can be upregulated by *pMesogenin1* (Fig. 4B). Additionally, in *Xenopus ESR4/5* are expressed in the tailbud domain where *pMesogenin1* is also expressed,

consistent with a positive regulatory relationship (either direct or indirect) between *pMesogenin1* and *ESR4/5* (Fig. 8; Jen *et al.*, 1999). Second, studies of a *MesP2* knockout in the mouse showed that the overall phenotype is disruption of segmentation and that, at the molecular level, elements of the *Notch* signaling pathway were disrupted in the knockout (Saga *et al.*, 1997). Moreover, *cMeso-1* and *Thylacine1/2* also play a functional role in segmentation, and in *Xenopus* their link to parts of the *Notch/Delta* signaling pathway has been shown (Buchberger *et al.*, 1998; Sparrow *et al.*, 1998). Third, the expression pattern for *pMesogenin1* and its relatives fits the bill for regulators that could govern expression of additional parts of the somitic clock, which include but are not limited to those that oscillate (Palmeirim *et al.*, 1997). Thus, *pMesogenin1* is specifically expressed throughout the caudal presomitic paraxial mesoderm domain in which the *cHairy1* and *Lunatic fringe* genes oscillate (Fig. 8B). This last possibility is highly speculative and we note that this expression domain is not unique to *pMesogenin1*, although *Tbx6* in the mouse is the only other gene known to us to be expressed in this pattern (Yoon and Wold, unpublished data; Chapman *et al.*, 1996). Taken together, these data from mammals and amphibians have led to a working model in which *pMesogenin1* and *MesP1/2* (*Thylacine1/2*) function, at least in part, to regulate expression of members of the *Notch/Delta* signaling pathway within presomitic paraxial mesoderm. This regulation may be direct or indirect and may include members of the oscillating clock set.

pMesogenin1 Regulatory Capacity and Specificity for Paraxial Mesoderm

We found that targets of *pMesogenin1* regulatory activity prominently include markers of future paraxial mesoderm such as *Xwnt-8, XMyoD, XMyf-5,* and *ESR4/5* (Figs. 4A and 4B). This is a first line of evidence that argues that *pMesogenin1* has a role in regulating paraxial mesoderm phenotype. These results are consistent with the domain of *pMesogenin1* expression and with the domains of expression for these marker genes. This interpretation was strengthened by the observation that overexpressed mouse or *Xenopus pMesogenin1* induced morphological and histological phenotypes previously associated with formation of ventrolateral mesoderm in the animal caps cultured for prolonged period (Fig. 4; Cunliffe and Smith, 1994). In a similarly consistent manner, *pMesogenin1* failed to induce *Thylacine2,* which is a marker of more mature somitomeres that do not normally express *pMesogenin1* (Figs. 4 and 8). Although a negative result such as the one for *Thylacine2* is inevitably less certain than is a marker gene induction, we speculate that ongoing ectopic expression of *pMesogenin1* may dictate an early paraxial mesoderm phenotype that precludes progression of ectopically expressing cells to a later (somitomeric) phenotype. We also note that one cannot conclude from the present study whether *pMesogenin1* can induce all aspects of the early (presomitomeric) unsegmented paraxial mesoderm, although it is sufficient to assay the ones we tested.

The ability of *pMesogenin1* to induce *Xwnt-8, XMyoD, XMyf-5,* and *ESR4/5* raises the possibility that the observed ability of *pMesogenin1* to direct animal cap explants to differentiate as ventrolateral mesoderm could be attributable to the activity of one or more of these induced regulatory genes. For example, ectopic expression of *Xwnt-8* after midblastula transition in animal caps promotes formation of ventrolateral mesoderm (Christian and Moon, 1993). In intact embryos *Xwnt-8* is necessary and sufficient for induction of *XMyoD* (Hoppler *et al.*, 1996) in a manner dependent upon BMP signaling (Hoppler and Moon, 1998). Moreover, dorsal expression of *Xwnt-8* after midblastula transition (Christian and Moon, 1993), like dorsal expression of *pMesogenin1,* abolishes formation of the notochord. Thus, *pMesogenin1* is likely to be an upstream activator of a set of regulatory genes that, in turn, promote ventrolateral cell fates.

A second related line of evidence that *pMesogenin1* plays a role in discriminating paraxial mesoderm from axial mesoderm is that markers specific for dorsal (future axial) mesoderm, *goosecoid* and *Chordin,* were absent or were present only at low levels (depending on the specific experiment) in the animal cap explants injected with *pMesogenin1* RNA (Fig. 4A). A third independent line of evidence in favor of paraxial mesoderm specificity is from embryo injection assays into the DMZ in which ectopically expressed *pMesogenin1* actively suppressed the expression of axial marker genes and structures (Fig. 5).

Interaction of pMesogenin1 with T-Box Genes

In functional assays several T-box transcription factors of *Xenopus* induce mesoderm that expresses both axial and nonaxial marker genes and phenotypes (Smith, 1999). We found that these genes can also be induced by ectopic *pMesogenin1* RNA in the animal cap assays (Figs. 4 and 7). They differ from the other mesodermal marker genes induced by *pMesogenin1* because they are normally expressed in a panmesodermal pattern that includes both dorsal and ventrolateral domains that later segregate axial from paraxial and lateral mesoderm (Fig. 6; Smith *et al.*, 1991; Zhang and King, 1996). In our animal cap explant experiments, ectopic *pMesogenin1* induced both *Xbra* and *VegT* RNAs very efficiently and *Eomesodermin* RNA weakly (Fig. 7). A simple interpretation is that the animal cap assay has uncovered a regulatory circuit in which expression of T-box regulators can be sustained or positively reinforced by *pMesogenin1* in the context of cells that are similar to nonaxial mesoderm. These T-box genes can themselves induce a panmesodermal phenotype, raising an apparent paradox. Why don't the panmesodermal T-box products induced by *pMesogenin1* RNA generate an additional dorsal (axial) phenotype? One explanation is that the levels of T-box factor expression induced by ectopic *pMesogenin1* may be insufficient to drive the full panmesodermal phe-

notype. However, another simple and perhaps more interesting explanation is that *Xwnt-8* and *pMesogenin1* can suppress axial mesodermal fates in whole-embryo injections, and they may be doing so in this cellular context as well.

ACKNOWLEDGMENTS

We thank Drs. John Gurdon, Mary Lou King, Chris Kintner, Marc Kirschner, Cheegun Lee, Eric Olson, Virginia Papaioannou, Yumiko Saga, Gerald Thomsen, and David Turner for providing their valuable reagents; Dr. Brian Williams for critically reading the manuscript; and Jason Chua for excellent technical assistance. We are greatly indebted to Drs. Scott Fraser and Marianne Bronner-Fraser for allowing us to use their *Xenopus* injection apparatus and to Dr. Maiyon Park for assistance at the beginning of this project. This work was supported by grants from NIH NIAMS to B.J.W. R.T.M. is supported as an Investigator of the HHMI.

Note added in proof. pMesogenin1 cDNA sequences have been submitted to GenBank. (Accession numbers are AF261105 for the mouse gene and AF261106 for the Xenopus gene, respectively.)

REFERENCES

Barnes, G. L., Alexander, P. G., Hsu, C. W., Mariani, B. D., and Tuan, R. S. (1997). Cloning and characterization of chicken Paraxis: A regulator of paraxial mesoderm development and somite formation. *Dev. Biol.* **189,** 95–111.

Beddington, R. A. S., and Smith, J. C. (1993). Control of vertebrate gastrulation: Inducing signals and responding genes. *Curr. Opin. Genet. Dev.* **3,** 655–661.

Buchberger, A., Seidl, K., Klein, C., Eberhardt, H., and Arnold, H. H. (1998). cMeso-1, a novel bHLH transcription factor, is involved in somite formation in chicken embryos. *Dev. Biol.* **199,** 201–215.

Burgess, R., Cserjesi, P., Ligon, K. L., and Olson, E. N. (1995). Paraxis—A basic helix-loop-helix protein expressed in paraxial mesoderm and developing somites. *Dev. Biol.* **168,** 296–306.

Burgess, R., Rawls, A., Brown, D., Bradley, A., and Olson, E. N. (1996). Requirement of the paraxis gene for somite formation and musculoskeletal patterning. *Nature* **384,** 570–573.

Chapman, D. L., Agulnik, I., Hancock, S., Silver, L. M., and Papaioannou, V. E. (1996). Tbx6, a mouse T-box gene implicated in paraxial mesoderm formation at gastrulation. *Dev. Biol.* **180,** 534–542.

Cho, K. W. Y., Blumberg, B., Steinbeisser, H., and Derobertis, E. M. (1991). Molecular nature of Spemanns organizer—The role of the Xenopus homeobox gene goosecoid. *Cell* **67,** 1111–1120.

Chomczynski, P., and Sacchi, N. (1987). Single-step method of RNA isolation by acid guanidinium thiocyanate phenol chloroform extraction. *Anal. Biochem.* **162,** 156–159.

Christ, B., and Ordahl, C. P. (1995). Early stages of chick somite development. *Anat. Embryol.* **191,** 381–396.

Christian, J. L., McMahon, J. A., McMahon, A. P., and Moon, R. T. (1991). Xwnt-8, a Xenopus Wnt-1/Int-1-related gene responsive to mesoderm-inducing growth-factors, may play a role in ventral mesodermal patterning during embryogenesis. *Development* **111,** 1045–1055.

Christian, J. L., and Moon, R. T. (1993). Interactions between Xwnt-8 and Spemann organizer signaling pathways generate dorsoventral pattern in the embryonic mesoderm of Xenopus. *Genes Dev.* **7,** 13–28.

Conlon, R. A., Reaume, A. G., and Rossant, J. (1995). Notch1 is required for the coordinate segmentation of somites. *Development* **121,** 1533–1545.

Cooke, J. (1998). A gene that resuscitates a theory—Somitogenesis and a molecular oscillator. *Trends Genet.* **14,** 85–88.

Cossu, G., Tajbakhsh, S., and Buckingham, M. (1996). How is myogenesis initiated in the embryo? *Trends Genet.* **12,** 218–223.

Cserjesi, P., Brown, D., Ligon, K. L., Lyons, G. E., Copeland, N. G., Gilbert, D. J., Jenkins, N. A., and Olson, E. N. (1995). Scleraxis—A basic helix-loop-helix protein that prefigures skeletal formation during mouse embryogenesis. *Development* **121,** 1099–1110.

Cunliffe, V., and Smith, J. C. (1994). Specification of mesodermal pattern in Xenopus laevis by interactions between Brachyury, Noggin and Xwnt-8. *EMBO J.* **13,** 349–359.

Dambly-Chaudiere, C., and Vervoort, M. (1998). The bHLH genes in neural development. *Int. J. Dev. Biol.* **42,** 269–273.

Dawid, I. B. (1991). Mesoderm induction. *In* "Methods in Cell Biology" (B. K. Kay and H. B. Peng, Eds.), Vol. 36, pp. 311–328. Academic Press, San Diego.

deAngelis, M. H., McIntyre, J., and Gossler, A. (1997). Maintenance of somite borders in mice requires the Delta homologue Dll-1. *Nature* **386,** 717–721.

del Barco Barrantes, I., Elia, A. J., Wunsch, K., De Angelis, M. H., Mak, T. W., Rossant, J., Conlon, R. A., Gossler, A., and de la Pompa, J. L. (1998). Interaction between Notch signalling and Lunatic fringe during somite boundary formation in the mouse. *Curr. Biol.* **9,** 470–480.

Evrard, Y. A., Lun, Y., Aulehla, A., Gan, L., and Johnson, R. L. (1998). Lunatic fringe is an essential mediator of somite segmentation and patterning. *Nature* **394,** 377–381.

Forsberg, H., Crozet, F., and Brown, N. A. (1998). Waves of mouse Lunatic fringe expression, in four-hour cycles at two-hour intervals, precede somite boundary formation. *Curr. Biol.* **8,** 1027–1030.

Gossler, A., and de Angelis, M. H. (1998). Somitogenesis. *In* "Current Topics in Developmental Biology" (R. A. Pedersen and G. P. Schatten, Eds.), Vol. 38, pp. 225–287. Academic Press, New York.

Henrique, D., Adam, J., Myat, A., Chitnis, A., Lewis, J., and Ishhorowicz, D. (1995). Expression of a Delta-homolog in prospective neurons in the chick. *Nature* **375,** 787–790.

Henthorn, P., Kiledjian, M., and Kadesch, T. (1990). Two distinct transcription factors that bind the immunoglobulin enhancer Mu-E5/Ke2 motif. *Science* **247,** 467–470.

Herrmann, B. G., Labeit, S., Poustka, A., King, T. R., and Lehrach, H. (1990). Cloning of the T-gene required in mesoderm formation in the mouse. *Nature* **343,** 617–622.

Hollenberg, S. M., Sternglanz, R., Cheng, P. F., and Weintraub, H. (1995). Identification of a new family of tissue-specific basic helix-loop-helix proteins with a two-hybrid system. *Mol. Cell. Biol.* **15,** 3813–3822.

Hoppler, S., Brown, J. D., and Moon, R. T. (1996). Expression of a dominant-negative Wnt blocks induction of MyoD in Xenopus embryos. *Genes Dev.* **10,** 2805–2817.

Hoppler, S., and Moon, R. T. (1998). BMP-2/-4 and Wnt-8 cooperatively pattern the Xenopus mesoderm. *Mech. Dev.* **71,** 119–129.

Hopwood, N. D., Pluck, A., and Gurdon, J. B. (1989). Myod expression in the forming somites is an early response to mesoderm induction in Xenopus embryos. *EMBO J.* **8,** 3409–3417.

Hopwood, N. D., Pluck, A., and Gurdon, J. B. (1991). Xenopus Myf-5 marks early muscle-cells and can activate muscle genes ectopically in early embryos. *Development* **111,** 551–560.

Horb, M. E., and Thomsen, G. H. (1997). A vegetally localized T-box transcription factor in Xenopus eggs specifies mesoderm and endoderm and is essential for embryonic mesoderm formation. *Development* **124,** 1689–1698.

Jacobson, A. G. (1993). Somitomeres: Mesodermal segments of the head and trunk. *In* "The Vertebrate Skull" (J. Hanken and B. Hall, Eds.), Vol. 1, pp. 42–76. Univ. of Chicago Press, Chicago.

Jen, W. C., Gawantka, V., Pollet, N., Niehrs, C., and Kintner, C. (1999). Periodic repression of Notch pathway genes governs the segmentation of Xenopus embryos. *Genes Dev.* **13,** 1486–1499.

Jen, W. C., Wettstein, D., Turner, D., Chitnis, A., and Kintner, C. (1997). The Notch ligand, X-Delta-2, mediates segmentation of the paraxial mesoderm in Xenopus embryos. *Development* **124,** 1169–1178.

Jiang, Y. J., Smithers, L., and Lewis, J. (1998). The clock is linked to Notch signalling. *Curr. Biol.* **8,** 868–871.

Joseph, E. M., and Cassetta, L. A. (1999). Mespo: A novel basic helix-loop-helix gene expressed in the presomitic mesoderm and posterior tailbud of Xenopus embryos. *Mech. Dev.* **82,** 191–194.

Kageyama, R., and Nakanishi, S. (1997). Helix-loop-helix factors in growth and differentiation of the vertebrate nervous system. *Curr. Opin. Genet. Dev.* **7,** 659–665.

Kelly, G. M., Eib, D. W., and Moon, R. T. (1991). Histological preparation of Xenopus laevis oocytes and embryos. *In* "Methods in Cell Biology" (B. K. Kay and H. B. Peng, Eds.), Vol. 36, pp. 389–417. Academic Press, San Diego.

King, M. W., Blackwood, E. M., and Eisenman, R. N. (1993). Expression of two distinct homologs of Xenopus Max during early development. *Cell Growth Differ.* **4,** 85–92.

Kusumi, K., Sun, E. S., Kerrebrock, A. W., Bronson, R. T., Chi, D. C., Bulotsky, M. S., Spencer, J. B., Birren, B. W., Frankel, W. N., and Lander, E. S. (1998). The mouse pudgy mutation disrupts Delta homologue Dll3 and initiation of early somite boundaries. *Nat. Genet.* **19,** 274–278.

Lawson, K. A., and Pedersen, R. A. (1992). Clonal analysis of cell fate during gastrulation and early neurulation in the mouse. *Ciba Found. Symp.* **165,** 3–26.

Li, L., Cserjesi, P., and Olson, E. N. (1995). Dermo-1—A novel Twist-related bHLH protein expressed in the developing dermis. *Dev. Biol.* **172,** 280–292.

Lustig, K. D., Kroll, K. L., Sun, E. E., and Kirschner, M. W. (1996). Expression cloning of a Xenopus T-related gene (Xombi) involved in mesodermal patterning and blastopore lip formation. *Development* **122,** 4001–4012.

McGrew, M. J., Kim Dale, J., Fraboulet, S., and Pourquie, O. (1998). The lunatic fringe gene is a target of the molecular clock linked to somite segmentation. *Curr. Biol.* **8,** 979–982.

Moon, R. T., and Christian, J. L. (1989). Microinjection and expression of synthetic mRNAs in Xenopus embryos. *J. Methods Cell Mol. Biol.* **1,** 76–89.

Palmeirim, I., Henrique, D., IshHorowicz, D., and Pourquie, O. (1997). Avian hairy gene expression identifies a molecular clock linked to vertebrate segmentation and somitogenesis. *Cell* **91,** 639–648.

Ryan, K., Garrett, N., Mitchell, A., and Gurdon, J. B. (1996). Eomesodermin, a key early gene in Xenopus mesoderm differentiation. *Cell* **87,** 989–1000.

Saga, Y., Hata, N., Kobayashi, S., Magnuson, T., Seldin, M. F., and Taketo, M. M. (1996). MesP1: A novel basic helix-loop-helix protein expressed in the nascent mesodermal cells during mouse gastrulation. *Development* **122,** 2769–2778.

Saga, Y., Hata, N., Koseki, H., and Taketo, M. M. (1997). Mesp2: A novel mouse gene expressed in the presegmented mesoderm and essential for segmentation initiation. *Genes Dev.* **11,** 1827–1839.

Sasai, Y., Lu, B., Steinbeisser, H., Geissert, D., Gont, L. K., and Derobertis, E. M. (1994). Xenopus Chordin—A novel dorsalizing factor-activated by organizer-specific homeobox genes. *Cell* **79,** 779–790.

Schoenwolf, G. C. (1999). Early patterning events in avian embryogenesis. *Dev. Biol.* **210,** 226–226.

Smith, J. (1999). T-box genes—What they do and how they do it. *Trends Genet.* **15,** 154–158.

Smith, J. C. (1995). Mesoderm-inducing factors and mesodermal patterning. *Curr. Opin. Cell Biol.* **7,** 856–861.

Smith, J. C., Price, B. M. J., Green, J. B. A., Weigel, D., and Herrmann, B. G. (1991). Expression of a Xenopus homolog of Brachyury (T) is an immediate-early response to mesoderm induction. *Cell* **67,** 79–87.

Smith, J. L., and Schoenwolf, G. C. (1998). Getting organized: New insights into the organizer of higher vertebrates. *In* "Current Topics in Developmental Biology" (R. A. Pedersen and G. P. Schatten, Eds.), Vol. 40, pp. 79–110. Academic Press, New York.

Sosic, D., BrandSaberi, B., Schmidt, C., Christ, B., and Olson, E. N. (1997). Regulation of paraxis expression and somite formation by ectoderm- and neural tube-derived signals. *Dev. Biol.* **185,** 229–243.

Sparrow, D. B., Jen, W. C., Kotecha, S., Towers, N., Kintner, C., and Mohun, T. J. (1998). Thylacine 1 is expressed segmentally within the paraxial mesoderm of the Xenopus embryo and interacts with the Notch pathway. *Development* **125,** 2041–2051.

Stennard, F., Carnac, G., and Gurdon, J. B. (1996). The Xenopus T-box gene, Antipodean, encodes a vegetally localised maternal mRNA and can trigger mesoderm formation. *Development* **122,** 4179–4188.

Swiatek, P. J., Lindsell, C. E., Franco del Amo, F., Weinmaster, G., and Gridley, T. (1994). Notch1 is essential for postimplantation development in mice. *Genes Dev.* **8,** 707–719.

Tam, P. P. L. (1998). Postimplantation mouse development: Whole embryo culture and micromanipulation. *Int. J. Dev. Biol.* **42,** 895–902.

Tam, P. P. L., and Beddington, R. S. P. (1992). Establishment and organization of germ layers in the gastrulating mouse embryo. *Ciba Found. Symp.* **165,** 27–49.

Tam, P. P. L., and Tan, S. S. (1992). The somitogenetic potential of cells in the primitive streak and the tail bud of the organogenesis-stage mouse embryo. *Development* **115,** 703–715.

Tam, P. P. L., and Trainor, P. A. (1994). Specification and segmentation of the paraxial mesoderm. *Anat. Embryol.* **189,** 275–305.

Yun, K. S., and Wold, B. (1996). Skeletal muscle determination and differentiation: Story of a core regulatory network and its context. *Curr. Opin. Cell Biol.* **8,** 877–889.

Zhang, J., and King, M. L. (1996). Xenopus VegT RNA is localized to the vegetal cortex during oogenesis and encodes a novel T-box transcription factor involved in mesodermal patterning. *Development* **122,** 4119–4129.

Zhang, N., and Gridley, T. (1998). Defects in somite formation in lunatic fringe-deficient mice. *Nature* **394,** 374–377.

Received for publication January 20, 2000
Revised March 16, 2000
Accepted March 21, 2000